DOI: 10.38103/jcmhch.18.3.8

Case report

VIRTUAL SURGICAL PLANNING AND 3D PRINTING IN NEOCONDYLE REGENERATION AFTER MANDIBULAR CONDYLE RECONSTRUCTION WITH MICROVASCULAR FIBULA FREE FLAP: REPORT OF TWO CLINICAL CASES

Nguyen Hong Loi[1], Nguyen Van Khanh[1], Ho Man Truong Phu[2]

[1]Center of Odonto - Stomatology, Hue Central Hospital, Vietnam

[2]Orthopedic Trauma Center, Hue Central Hospital, Vietnam

ABSTRACT

Background: *Mandibular condyle reconstruction remains a challenging procedure because it requires restoration of mandibular continuity, occlusion, facial symmetry, and temporomandibular joint function. Virtual surgical planning (VSP) and three-dimensional (3D) printing may improve the precision of fibula free flap reconstruction and facilitate accurate neocondyle positioning.*

Case presentation: *We report two female patients who underwent segmental mandibulectomy involving the condylar region followed by microvascular fibula free flap reconstruction assisted by VSP and 3D printing. The first patient was a 35-year-old woman with fibrous dysplasia and an approximately 13-cm mandibular defect. A three-segment fibula reconstruction was performed, with preservation of the articular disc and passive positioning of the distal fibular end as a neocondyle. The second patient was a 65-year-old woman with unicystic ameloblastoma and an approximately 11-cm mandibular defect. A two-segment fibula reconstruction was performed, and the distal fibular end was positioned approximately 3 mm below the glenoid fossa. Operative time was 5.5 hours and 5 hours, respectively. During follow-up at 3, 6, 12, and 18 months, both patients showed stable mandibular contour, acceptable occlusion, satisfactory mouth opening, and no temporomandibular joint ankylosis or tumor recurrence. Serial imaging demonstrated adaptive remodeling of the distal fibular end into a neocondyle-like structure, with bone growth mainly directed along the lateral pterygoid traction vector and toward the glenoid fossa. The younger patient showed more pronounced remodeling than the older patient.*

Conclusion: *VSP and 3D printing enabled accurate planning and transfer of fibula osteotomies, supported passive neocondyle positioning, and contributed to stable functional reconstruction after mandibular condyle resection. Neocondyle regeneration after fibula free flap reconstruction appears to be functionally driven by muscle traction and adaptive loading, although larger studies with quantitative 3D analysis are needed to confirm these findings.*

Keywords: *Virtual surgical planning; 3D printing; fibula free flap; neocondyle regeneration; mandibular reconstruction; temporomandibular joint; lateral pterygoid muscle.*

I. INTRODUCTION

Mandibular defects involving the condyle are among the most difficult reconstructive problems in oral and maxillofacial surgery. In addition to replacing the resected bone, reconstruction must restore vertical ramus height, mandibular contour, centric occlusion, facial symmetry, masticatory function, and a stable relationship with the glenoid fossa. Failure to achieve a functional condylar unit may result in deviation during mouth opening,

Received: 17/12/2025. **Revised:** 27/02/2026. **Accepted:** 05/5/2026.

Corresponding author: Nguyen Van Khanh. Email: drkhanhrhm@gmail.com. Phone: (+84) 935884886

malocclusion, temporomandibular pain, ankylosis, or progressive temporofibular changes.

Several methods have been used for condylar reconstruction, including costochondral grafts, distraction osteogenesis, sternoclavicular grafts, alloplastic TMJ prostheses, and vascularized bone transfer. For long composite mandibular defects, the vascularized fibula free flap remains a reliable option because it provides sufficient bone length, a long vascular pedicle, robust cortical bone, and the possibility of multiple osteotomies while maintaining vascularity [1-3].

However, condylar reconstruction with a fibula free flap is technically sensitive. The distal fibular segment must be placed in a position that is sufficiently close to the glenoid fossa to maintain mandibular height and guidance, but not so close as to create direct traumatic contact with the fossa or articular disc. Preservation of the articular disc, passive seating of the distal fibula, guided occlusion, and early functional mobilization have been emphasized as important factors for avoiding ankylosis and promoting adaptive neocondyle remodeling [1, 4].

VSP and 3D printing provide a digital workflow for segmenting the mandible and fibula, simulating resection, designing osteotomies, and fabricating patient-specific cutting guides and biomodels. These tools may improve the transfer of the virtual plan to the operating room, reduce intraoperative trial-and-error contouring, shorten operative time, and improve mandibular symmetry [5-9]. This report presents two cases of mandibular condyle reconstruction using VSP- and 3D-printing-assisted microvascular fibula free flap reconstruction, with emphasis on long-term distal fibular remodeling and neocondyle bone regeneration.

II. CASE REPORTS

2.1. Preoperative digital planning and operative workflow

Both patients underwent clinical examination, occlusal assessment, and preoperative maxillofacial CT or cone-beam CT to define the extent of mandibular involvement. Lower limb vascular evaluation was performed before fibula harvest. DICOM data were imported into digital planning software for 3D segmentation of the mandible, lesion, glenoid fossa, residual dental arch, and fibula.

The planned mandibular resection was simulated virtually. The fibula was then positioned to restore mandibular continuity, ramus height, lower facial contour, and distal neocondyle alignment. Three-dimensional printed biomodels and cutting guides were used intraoperatively to reproduce the planned osteotomies. The distal fibular end was designed to function as a neocondyle. In both cases, the articular disc was preserved when technically feasible, and the distal fibular segment was passively positioned in the joint space without forced impaction against the glenoid fossa. Occlusion was guided postoperatively using elastics or intermaxillary fixation according to the clinical situation.

2.2. Case 1

A 35-year-old female patient presented with a large mandibular lesion diagnosed as fibrous dysplasia. Imaging demonstrated mandibular involvement requiring segmental mandibulectomy including the condylar region. The expected bony defect was approximately 13 cm. The treatment goal was to remove the diseased mandibular segment while reconstructing mandibular continuity, ramus height, occlusion, and TMJ function.

Using VSP, the resection was simulated and the fibula free flap was planned as a three-segment reconstruction to reproduce the mandibular curvature and condylar height. The articular disc was preserved. After segmental mandibulectomy and fibula harvest, the fibula was osteotomized according to the 3D-printed guide. The distal fibular segment was positioned as a neocondyle under the preserved disc and passively seated within the joint space. The total operative time was 5.5 hours.

The flap survived without major early complications. Guided occlusion was maintained during the early healing phase. At 3 months, the patient achieved a maximum mouth opening of approximately 35 mm. Serial follow-up at 3, 6, 12, and 18 months showed stable mandibular reconstruction, satisfactory facial symmetry, acceptable occlusion, and no TMJ ankylosis. Radiographic assessment showed progressive rounding and adaptive remodeling of the distal fibular end, with greater neocondylar bone development than in the older patient. The preoperative assessment and virtual surgical planning are presented in Figure 1, the early postoperative radiographic and functional outcomes in Figure 2, and serial neocondylar remodeling in Figure 3.

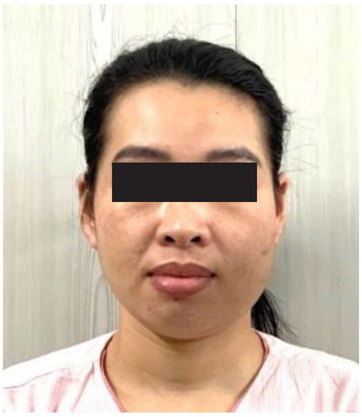

A. Preoperative frontal view

B. Preoperative occlusion

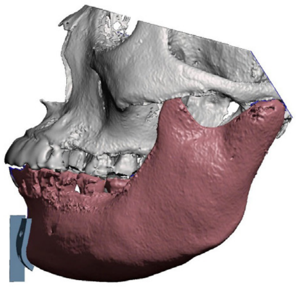

C. 3D reconstruction of the mandibular lesion

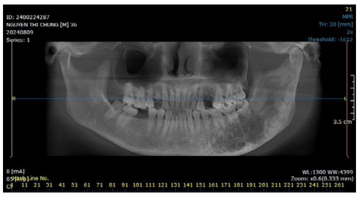

D. Preoperative panoramic radiograph

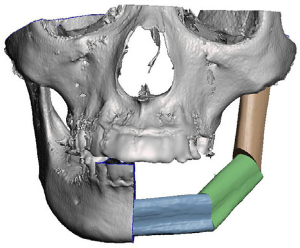

E. Virtual mandibular reconstruction plan

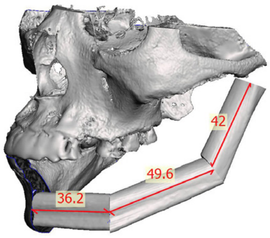

F. Planned fibular segmentation and neocondyle position

Figure 1: Case 1. Preoperative assessment and virtual surgical planning in a 35-year-old female patient with fibrous dysplasia, showing the mandibular lesion involving the ramus-condylar region, planned segmental resection, three-segment fibular reconstruction, and planned distal fibular neocondyle position.

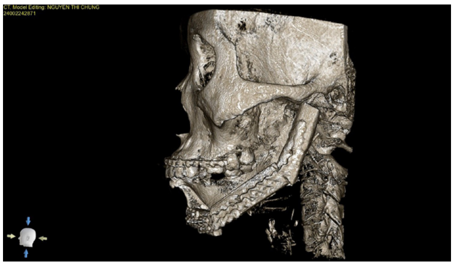

A. Early postoperative 3D reconstruction

B. Postoperative panoramic radiograph

C. Mouth opening during follow-up

D. Guided occlusion during early rehabilitation

Figure 2: Case 1. Postoperative radiographic and functional outcomes showing stable fibula free flap reconstruction, satisfactory occlusion, mouth opening recovery, and no evidence of temporomandibular ankylosis.

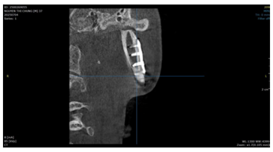
A. 3-month CT/CBCT follow-up

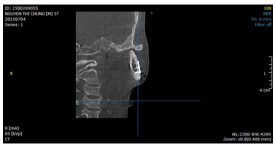
B. 6-month CT/CBCT follow-up

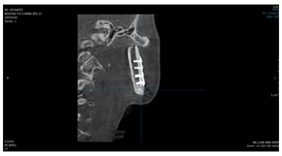
C. 12-month CT/CBCT follow-up

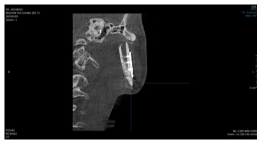
D. 18-month CT/CBCT follow-up

Figure 3: Case 1. Serial postoperative CT/CBCT follow-up demonstrating progressive remodeling and rounding of the distal fibular segment into a neocondyle-like structure at 3, 6, 12, and 18 months.

2.3. Case 2

A 65-year-old female patient was diagnosed with unicystic ameloblastoma involving the mandibular segment and condylar region. The planned segmental mandibulectomy resulted in an estimated 11-cm defect. The reconstructive objective was to restore mandibular continuity and TMJ function while minimizing the risk of neocondyle malposition, ankylosis, and facial asymmetry.

VSP was used to determine the extent of resection and the fibular osteotomy design. The fibula was contoured into two segments. The articular disc was preserved. The distal fibular segment was positioned approximately 3 mm below the glenoid fossa to preserve a functional joint space and avoid direct traumatic contact with the temporal bone. The total operative time was 5 hours.

The postoperative course was favorable. Mouth opening improved during the first 3 months and was clinically satisfactory; because an exact maximum mouth opening value was not available in the follow-up record, this outcome was reported qualitatively. From the 6-month follow-up, CT/CBCT showed neocondyle-like bone formation at the distal end of the fibula. At 12 and 18 months, mandibular contour and occlusion remained stable. No TMJ ankylosis or clinical recurrence was observed. Compared with Case 1, bone growth was present but less pronounced, consistent with lower remodeling potential in an older patient. The preoperative assessment and virtual surgical planning are shown in Figure 4, the postoperative functional and radiographic outcomes in Figure 5, and follow-up neocondylar adaptation in Figure 6.


A. Preoperative occlusion

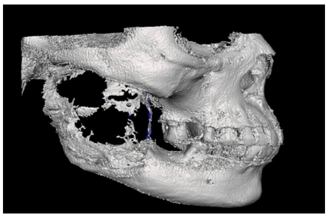
B. Lateral 3D CT/CBCT reconstruction


C. Frontal 3D CT/CBCT reconstruction

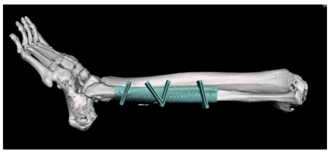
D. Planned fibular osteotomy

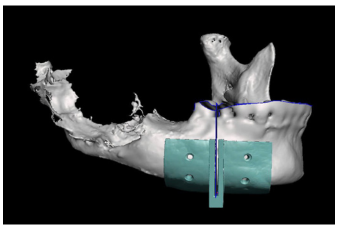
E. Planned mandibular resection and fibular inset

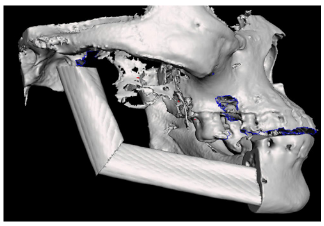
F. Planned distal fibular neocondyle position below the glenoid fossa

Figure 4: Case 2. Preoperative assessment and virtual surgical planning in a 65-year-old female patient with unicystic ameloblastoma, showing the mandibular lesion, two-segment fibular reconstruction, and planned positioning of the distal fibular segment approximately 3 mm below the glenoid fossa

A. Postoperative occlusion

B. Maximum mouth opening during follow-up

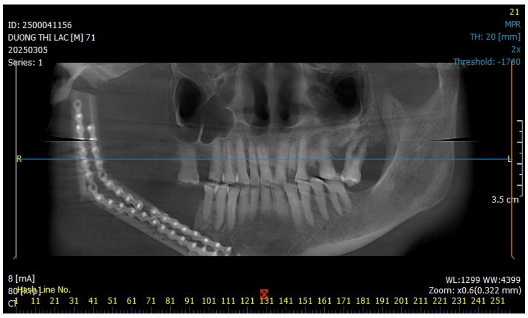

C. Postoperative panoramic radiograph

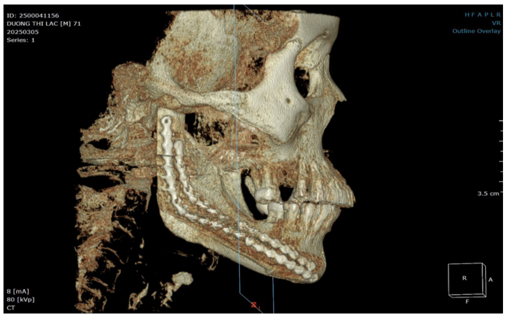

D. Postoperative 3D reconstruction

Figure 5: Case 2. Postoperative functional and radiographic outcomes showing acceptable occlusion, satisfactory mouth opening, stable fibula free flap fixation, and appropriate distal fibular neocondyle position

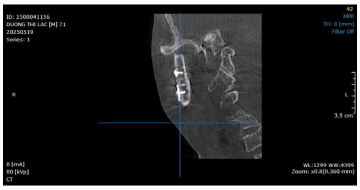

A. Sagittal CT/CBCT view of the distal fibular segment

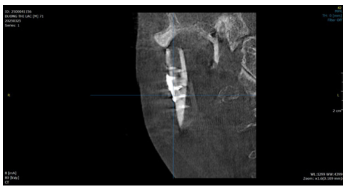

B. Follow-up CT/CBCT view showing distal fibular adaptation

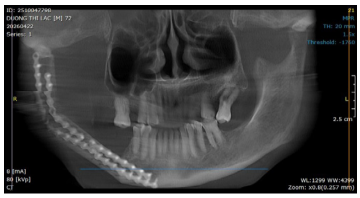

C. Follow-up panoramic radiograph showing stable reconstruction

Figure 6: Case 2. Follow-up CT/CBCT and panoramic imaging showing stable distal fibular neocondyle position, adaptive remodeling, and maintenance of mandibular reconstruction without ankylosis

2.4. Comparative clinical and surgical summary

The clinical and surgical characteristics of both patients are summarized in Table 1, and long-term distal fibular neocondyle remodeling is presented in Table 2.

Table 1: Clinical and surgical summary of the two cases.

Variable	Case 1	Case 2
Age/sex	35-year-old female	65-year-old female
Diagnosis	Fibrous dysplasia	Unicystic ameloblastoma
Mandibular defect length	Approximately 13 cm	Approximately 11 cm
Resection	Segmental mandibulectomy including the condylar region	Segmental mandibulectomy including the condylar region

Variable	Case 1	Case 2
Fibula flap design	Three-segment fibula reconstruction	Two-segment fibula reconstruction
Articular disc	Preserved	Preserved
Neocondyle positioning	Distal fibular end passively positioned under the disc within the joint space	Distal fibular end positioned approximately 3 mm below the glenoid fossa
Digital technique	VSP, 3D biomodel, and 3D-printed osteotomy guide	VSP, 3D biomodel, and 3D-printed osteotomy guide
Operative time	5.5 hours	5 hours
Early functional result	Maximum mouth opening 35 mm at 3 months	Clinically satisfactory mouth opening from 3 months; exact MMO value not available
Radiographic remodeling	Progressive rounding and higher neocondyle-like bone formation	Neocondyle-like bone formation from 6 months, less than Case 1
Follow-up outcome	Stable reconstruction at 3, 6, 12, and 18 months; no ankylosis	Stable reconstruction at 3, 6, 12, and 18 months; no ankylosis

Table 2: Long-term follow-up of distal fibular neocondyle remodeling and bone regeneration

Parameter	Case 1: 35-year-old fibrous dysplasia	Case 2: 65-year-old unicystic ameloblastoma	Interpretation
3 months	Stable neocondyle position; distal fibular end begins rounding; MMO approximately 35 mm	Stable reconstruction; clinically satisfactory mouth opening; early adaptive remodeling	Early function and passive joint-space seating are maintained
6 months	Radiographic stability; more evident distal fibular remodeling	Clear neocondyle-like bone formation from the distal fibular end	Average time to functional and radiographic stability: approximately 6 months
12 months	Stable occlusion and facial symmetry; maturation of neocondyle contour	Stable occlusion and mandibular contour; maturation of neocondyle-like bone	Adaptive remodeling continues after initial stabilization
18 months	Stable reconstruction; no ankylosis; no clinical recurrence	Stable reconstruction; no ankylosis; no clinical recurrence	Both cases achieved favorable mid-term outcomes
Main direction of bone growth	Along the lateral pterygoid traction vector and toward the glenoid fossa	Along the lateral pterygoid traction vector and toward the glenoid fossa	Two dominant remodeling directions are consistent with 3D morphologic observations in the literature

Parameter	Case 1: 35-year-old fibrous dysplasia	Case 2: 65-year-old unicystic ameloblastoma	Interpretation
Newly formed bone volume	Greater than the older patient; included in the two-case mean of 0.39 cm^3	Lower than the younger patient; included in the two-case mean of 0.39 cm^3	Mean newly formed bone volume across both cases: 0.39 cm^3
Age-related observation	Greater remodeling potential	Lower remodeling potential	Younger patients may show stronger neocondylar bone regeneration than elderly patients

III. DISCUSSION

The present two cases show that mandibular condyle reconstruction with a microvascular fibula free flap can provide not only skeletal continuity but also adaptive neocondyle regeneration when the distal fibular end is accurately positioned and functionally loaded. In condylar reconstruction, the surgical objective is different from simple mandibular bridging. The reconstruction must recreate a biologically viable and mechanically guided condylar unit that maintains ramus height, occlusion, facial symmetry, and mandibular movement.

The most important observation in this report is the long-term remodeling of the distal end of the fibula into a neocondyle-like structure. This phenomenon supports the concept that the transferred fibula is not a static bone strut. After revascularization and functional loading, the distal fibular segment may undergo adaptive bone remodeling in response to muscle traction, occlusal guidance, and the spatial relationship with the glenoid fossa. Yu et al. reported that neocondyle bone growth after fibula free flap reconstruction occurs mainly in two directions: in the direction of lateral pterygoid traction and toward the glenoid fossa [4]. Our observations are consistent with this pattern. In both cases, bone formation was directed not only superiorly toward the fossa but also along the functional traction vector of the lateral pterygoid muscle.

The lateral pterygoid muscle may play a central biological and mechanical role in this process. Its traction may create a distraction-like stimulus at the distal fibular end, while the preserved disc and guided occlusion provide a soft-tissue interface and functional direction for remodeling. In this setting, neocondyle formation may be understood as a combined process of vascularized bone biology, mechanical loading, and joint-space adaptation. This mechanism is clinically meaningful because it explains why passive positioning, preservation of the disc, avoidance of direct bone-to-bone contact, and early mobilization are important technical details rather than minor operative preferences.

Age may influence the degree of neocondylar bone regeneration. In our two cases, the 35-year-old patient demonstrated greater distal fibular bone remodeling than the 65-year-old patient, although both patients achieved stable reconstruction and acceptable function. The average newly formed bone volume across the two cases was 0.39 cm^3. This finding should be interpreted cautiously because the sample size is small, but it suggests that host regenerative capacity may be an important determinant of postoperative neocondyle formation. Younger patients, especially children and young adults, may have greater bone remodeling potential than older adults; however, this hypothesis should be confirmed by larger prospective studies with standardized 3D volumetric analysis.

Preservation of the articular disc was a key surgical principle in both cases. The disc provides a biological spacer between the temporal bone and the distal fibular segment, reducing the risk of direct contact and temporofibular ankylosis. Park et al. emphasized that preservation of the disc, trapezoidal shaping of the distal fibular end, passive seating of the neocondyle, and guided occlusion are important factors for neocondyle remodeling without ankylosis [1]. Our approach followed the same concept. In Case 2, the distal fibular segment was intentionally positioned approximately 3 mm below the glenoid fossa to preserve a functional joint space and to avoid excessive pressure on the temporal bone.

VSP and 3D printing were essential to translating these biological principles into a precise surgical reconstruction. Preoperative digital planning allowed the team to determine resection limits, fibular segment number, osteotomy angles, ramus height, and distal neocondyle position before entering the operating room. Three-dimensional printed guides reduced intraoperative uncertainty and minimized repeated manual shaping of the fibula. This is particularly important in condylar reconstruction, where small positional errors may affect occlusion, mandibular deviation, facial symmetry, and the risk of ankylosis.

The operative time in our cases was 5.5 hours and 5 hours, respectively. These times are favorable for complex mandibular reconstruction involving the condylar region. Although this two-case report cannot prove superiority over conventional surgery, our experience supports the practical value of VSP and 3D-printed guides in reducing intraoperative decision-making, improving the accuracy of osteotomy transfer, and facilitating flap inset. Recent studies have similarly reported that VSP and 3D printing may improve facial symmetry, increase surgical reproducibility, reduce operative time in selected settings, and improve the precision of fibular utilization [5-10].

A shorter and more predictable operation may also have postoperative advantages. Because length of hospital stay was not formally analyzed or compared in this report, the possible effect of VSP on postoperative recovery and hospitalization should be interpreted only as a hypothesis for future evaluation. Future studies should include operative time, ischemia time, blood loss, length of stay, complications, functional rehabilitation, and 3D accuracy as predefined outcomes.

Several technical recommendations can be drawn from these cases: (1) perform careful CT/CBCT-based 3D segmentation of the lesion, mandible, glenoid fossa, and fibula; (2) preserve the articular disc whenever oncologically safe; (3) design the distal fibular end as a passive neocondyle rather than a forcefully seated condylar substitute; (4) maintain a small functional joint space; (5) use guided occlusion or intermaxillary fixation during early healing; (6) begin mouth-opening exercises when safe; and (7) evaluate neocondyle remodeling using serial CT/CBCT at 3, 6, 12, and 18 months.

This report has limitations. It includes only two patients, both of whom were adults and had benign mandibular disease. Individual volumetric values of newly formed bone should be confirmed with standardized segmentation protocols and interobserver validation. Longer follow-up is required to determine whether the neocondyle remains stable beyond 18 months and whether remodeling continues or plate-related complications occur. Nevertheless, the combination of favorable clinical outcomes, radiographic remodeling, and absence of ankylosis suggests that VSP-assisted fibula free flap reconstruction is a promising approach for mandibular condyle reconstruction.

IV. CONCLUSION

Mandibular condyle reconstruction with a microvascular fibula free flap assisted by VSP and 3D printing achieved stable functional and aesthetic outcomes in two clinical cases. The technique enabled accurate preoperative simulation, precise transfer of fibular osteotomies, passive positioning of the distal fibular neocondyle, and favorable mid-term remodeling without TMJ ankylosis. Neocondyle bone growth occurred mainly under the influence of lateral pterygoid muscle traction and adaptive remodeling toward the glenoid fossa. The younger patient showed greater bone development than the older patient, suggesting that age-related regenerative capacity may influence neocondyle formation. In this two-case report, VSP and 3D printing appeared to streamline intraoperative decision-making, improve surgical accuracy, reduce intraoperative uncertainty, and support earlier postoperative stabilization. Larger comparative studies with standardized 3D volumetric analysis are required to determine whether these tools reduce operative time, ischemia time, and length of hospital stay.

Conflict of interest

The authors declare that they have no conflict of interest.

REFERENCES

1. Park HI, Chang HJ, Lee JH. Bone remodeling of the fibula segment as a form of neocondyle after free vascularized bone transfer: a report of two cases. J Korean Assoc Oral Maxillofac Surg. 2023; 49(6): 354-359.
2. May MM, Howe BM, O'Byrne TJ, Alexander AE, Morris JM, Moore EJ, et al. Short and long-term outcomes of three-dimensional printed surgical guides and virtual surgical planning versus conventional methods for fibula free flap reconstruction of the mandible: Decreased nonunion and complication rates. Head Neck. 2021; 43(8): 2342-2352.
3. Xu Y, Li Y, Xiao W, Yue J, Xue L, Li L, et al. Virtual surgical planning/3D printing assisted fibula osteoseptocutaneous flap combined with anterolateral thigh flaps for extensive composite oromandibular defects reconstruction: a retrospective study of case series. Front Bioeng Biotechnol. 2023; 11: 1273318.
4. Yu Y, Soh HY, Bai S, Zhang WB, Wang Y, Peng X. Three-dimensional morphological analysis of neocondyle bone growth after fibula free flap reconstruction. Int J Oral Maxillofac Surg. 2021; 50(11): 1429-1434.
5. Ritschl LM, Kilbertus P, Grill FD, Schwarz M, Weitz J, Nieberler M, et al. In-House, Open-Source 3D-Software-Based, CAD/CAM-Planned Mandibular Reconstructions in 20 Consecutive Free Fibula Flap Cases: An Explorative Cross-Sectional Study With Three-Dimensional Performance Analysis. Front Oncol. 2021; 11: 731336.
6. Garza-Cisneros AN, Garc├¡a-P├─rez MM, Rodriguez-Guajardo WJ, Elizondo-Riojas G, Negreros-Osuna AA. Cost-effective Solution for Maxillofacial Reconstruction Surgery with Virtual Surgical Planning and 3D Printed Cutting Guides Reduces Operative Time. Plast Surg (Oakv). 2024; 32(1): 70-77.
7. Garajei A, Modarresi A, Arabkheradmand A, Shirkhoda M. Functional and esthetic outcomes of virtual surgical planning versus the conventional technique in mandibular reconstruction with a free fibula flap: A retrospective study of 24 cases. J Craniomaxillofac Surg. 2024; 52(4): 454-463.
8. Villarm A, Pace-Loscos T, Schiappa R, Poissonnet G, Dassonville O, Chamorey E, et al. Impact of virtual surgical planning and three-dimensional modeling on time to surgery in mandibular reconstruction by free fibula flap. Eur J Surg Oncol. 2024; 50(3): 108008.
9. Tatti M, Carta F, Bontempi M, Deriu S, Mariani C, Marrosu V, et al. Segmental Mandibulectomy and Mandibular Reconstruction with Fibula-Free Flap Using a 3D Template. J Pers Med. 2024; 14(5).
10. Jiang L, Lin H, Shao Z, Liu B, Ge Z, Dai L, et al. Efficacy of personalized 3D-printed osteotomy guide in maximizing fibular utilization and minimizing graft length for reconstruction of large mandibular defect. Clin Oral Investig. 2024; 28(2): 125.